Hydrogen Exchange Shows Peptide Binding Stabilizes Motions in Hck SH2†

John R. Engen,‡ William H. Gmeiner,§ Thomas E. Smithgall,§,|| and David L. Smith*,‡,§

Department of Chemistry, University of Nebraska−Lincoln, Lincoln, Nebraska 68588-0304, and Eppley Institute for Research in Cancer and Allied Diseases, University of Nebraska Medical Center, Omaha, Nebraska 68198-6805

Received November 3, 1998; Revised Manuscript Received April 27, 1999

ABSTRACT: Src-homology-2 domains are small, 100 amino acid protein modules that are present in a number of signal transduction proteins. Previous NMR studies of SH2 domain dynamics indicate that peptide binding decreases protein motions in the pico- to nanosecond, and perhaps slower, time range. We suggest that amide hydrogen exchange and mass spectrometry may be useful for detecting changes in protein dynamics because hydrogen exchange rates are relatively insensitive to the time domains of the dynamics. In the present study, hydrogen exchange and mass spectrometry were used to probe hematopoietic cell kinase SH2 that was either free or bound to a 12-residue high-affinity peptide. Hydrogen exchange rates were determined by exposing free and bound SH2 to D_2O, fragmenting the SH2 with pepsin, and determining the deuterium level in the peptic fragments. Binding generally decreased hydrogen exchange along much of the SH2 backbone, indicating a widespread reduction in dynamics. Alterations in the exchange of the most rapidly exchanging amide hydrogens, which was detected following acid quench and analysis by mass spectrometry, were used to locate differences in low-amplitude motion when SH2 was bound to the peptide. In addition, the results indicate that hydrogen exchange from the folded form of SH2 is an important process along the entire SH2 backbone.

Proteins are not static structures. Their movement(s) are critical for carrying out normal cellular processes. From a more physical perspective, proteins have many very similar conformations that make up the native state. To characterize motion within proteins, we must study the interconversion of these folded states as well as the formation of normal but briefly populated unfolded states. Information about the dynamics of proteins can increase our understanding of the mechanisms by which proteins fold, unfold, and perform their normal activities. The dynamics of the Src-homology-2 (SH2[1]) domain from hematopoietic cell kinase (Hck) are being studied in an effort to understand the consequences of binding on protein motion(s).

Src-homology-2 domains are discrete protein modules of approximately 100 amino acids that have been widely studied [see refs *1, 2* for a review]. They are found in many proteins involved in intracellular signaling pathways, including the Src family of nonreceptor protein tyrosine kinases. X-ray crystal structures and NMR solution structures of SH2 domains from a variety of proteins have been determined, both in the free form and complexed to various ligands. A consensus structure consisting of a central triple-stranded β-sheet and a smaller double-stranded β-sheet, both flanked by two α-helices, creates two well-defined pockets into which a phosphotyrosine and a hydrophobic residue (frequently Ile or Leu in class I ligands) from a ligand may bind. Src family SH2 domains bind most tightly to ligands containing the sequence (pY)EEI. This binding has been compared to a two-holed socket engaging a two-pronged plug (*3*).

Ligand binding may alter protein dynamics over a wide time scale (picoseconds to minutes). Although various spectroscopic methods have been used to investigate protein dynamics, NMR has been most useful for linking structure and dynamics. Advantages offered by NMR in studying this wide time scale of motions include: (A) Assessment of changes in internal motion in the pico- to nanosecond time scale with ligand binding may be determined by comparing average order parameters (S^2) (*4, 5*) for free versus complexed proteins. Studies of this nature have been reported for numerous proteins [e.g., calbindin (*6*), staph nuclease (*7*), and various SH2 domains (*8*−*11*)]. (B) Conformational fluctuations on the micro to millisecond time scale can be probed with $R_{1\rho}-R_1$ constant-relaxation time ^{15}N nuclear spin relaxation experiments (*12*). (C) Hydrogen exchange (HX) combined with NMR can reveal information about protein dynamics, including localized unfolding rates (*13*) and the effects of ligand binding. Examples of the latter include protein−ligand complexes of cytochrome *c* (*14*), lysozyme

† This work was supported by NIH grant R01 GM40384 [D.L.S.], NIH grant R01 CA81398 [T.E.S.], NIH grant R01 60612 [W.H.G.], NIH grant P30 CA36727, the Nebraska Department of Health, and the Nebraska Center for Mass Spectrometry.

* To whom correspondence should be addressed: Department of Chemistry, University of Nebraska−Lincoln, Lincoln, NE 68588-0304. Telephone (402) 472−2794. Fax (402) 472−9402. E-mail: dsmith7@une.edu.

‡ University of Nebraska-Lincoln.

§ Eppley Institute.

|| Present address: Department of Molecular Genetics and Biochemistry, University of Pittsburgh School of Medicine, E1240 Biomedical Science Tower, Pittsburgh, PA 15261.

[1] Abbreviations: HX, hydrogen exchange; MS, mass spectrometry; NMR, nuclear magnetic resonance; ESIMS, electrospray ionization mass spectrometry; Hck, hematopoietic cell kinase; SH2, Src homology 2; SH3, Src homology 3; YEEI, phosphorylated SH2 ligand (AcNH-EPQpYEEIPIYL-COOH) from hamster middle T antigen; NH, amide hydrogen.

10.1021/bi982611y CCC: $18.00
Published on Web 06/18/1999

(*15*, *16*), serine-protease inhibitor (*17*), staph nuclease (*18*), barnase (*19*), protein G (*20*), and the acyl coenzyme A binding protein (*21*).

Hydrogen exchange rates in protein−ligand complexes can also be measured with mass spectrometry (MS) (*22*−*24*). As in the case for NMR, such hydrogen exchange information can be used to investigate protein dynamics. Detecting HX by mass spectrometry (HX/MS) is attractive because it can distinguish between cooperative and noncooperative isotope exchange (i.e., EX1 versus EX2 kinetics). HX/MS can also be used to determine HX rates for rapidly exchanging amide hydrogens at the surface of proteins (*25*), which may be important for both ligand binding and protein dynamics studies. In addition, HX/MS can be performed at concentrations well below those required for NMR measurements. This feature is important for studies of SH2 domains because they have been observed to form dimers or multimers at concentrations typically used for NMR (*8*−*11*) thus confounding interpretation of the data.

Motions in the pico- to nanosecond time range observed with NMR for several SH2 domains alone and in peptide complexes (*8*−*11*) indicated that motions slower than nanoseconds may be significant. This conclusion was reached because R_{ex} terms, which have been correlated with exchange between different conformations of the molecule (*12*), were required to fit the NMR relaxation data for many residues. To determine if slower motions might be affected by peptide binding, we have used HX/MS to investigate the dynamics of Hck SH2. Because hydrogen exchange rates are relatively insensitive to the time scale of protein dynamics, we may anticipate detecting changes in both fast (microseconds to milliseconds scale) and slow (seconds to hours) dynamics. The present results also lead to the identification of regions in which the SH2 unfolding dynamics are altered by peptide binding. Both solution (*26*) and crystal structures (*27*) of Hck SH2 have been reported allowing localization of HX/MS data to specific parts of the tertiary structure. In addition, the effects of peptide binding to Hck SH2 have been determined with NMR (*11*), thereby facilitating a comparison of dynamics assessed by the two methods.

MATERIALS AND METHODS

Materials. Recombinant Hck SH2 was expressed and purified as described (*28*). Briefly, a cDNA fragment encoding residues 119−224 of human *hck* was amplified with PCR, inserted into the bacterial expression vector pET-14b (Novagen), and transformed into *Escherichia coli* strain BL21(DE3)pLysS. Following purification by cation exchange and gel filtration chromatography, the protein was >95% pure by SDS−PAGE. The average molecular mass determined by ESIMS was 12 223 Da (calculated value 12 223 Da). Purified protein was lyophilized and stored at −70 °C. The phosphorylated YEEI peptide (AcNH-EPQpYEEIPIYL-COOH) from hamster middle T antigen was synthesized by the Alberta Peptide Institute and purified (>95%) by reversed phase HPLC. Its molecular mass was verified by ESIMS. Fully deuterated Hck SH2 (all exchangeable hydrogens replaced with deuterium) was prepared by incubating SH2 in 5 mM phosphate buffer, D_2O, pH 6.9 for 5 h at 37 °C followed by incubation for 24 h at room temperature, pH 6.9.

Deuterium Exchange into SH2. Hydrogen exchange experiments were similar to those reported previously (*24*). For analysis of the SH2 domain alone, SH2 (1600 pmol/μL) was allowed to equilibrate for 100 min at 22 °C in 10 μL of 5 mM phosphate buffer, pH 6.9, H_2O (equilibration solution). Deuterium exchange was initiated by diluting the equilibration solution 15-fold with 5 mM phosphate buffer, pH 6.9, D_2O (labeling solution). At each time point, ∼1.5 nmol of SH2 was removed from the labeling solution, diluted 1:1 with 100 mM phosphate buffer, pH 2.5, H_2O to quench isotopic exchange, and placed at −70 °C until analysis. This equilibration solution was adequate to prepare samples for analysis at 16 time points. For studies of SH2 binding to the YEEI peptide, ∼14 nmol of SH2 was dissolved into 10 μL of a YEEI solution (1600 pmol/μL in 5 mM phosphate buffer, pH 6.9, H_2O) and equilibrated and labeled as above for SH2 alone. For a K_d of 5 nM, 99% of the SH2 was expected to be bound. A K_d value of 5 nM is in the range of previously reported K_d values for the YEEI peptide and homologous SH2 domains (*29*−*31*).

The concentration of Hck SH2 in these experiments was 100 μM, well below the value at which NMR data were acquired on the same system (*11*). The lower concentration minimizes the possibility of forming dimers or multimers of SH2. Various SH2 domains were shown to form dimers or higher-order multimers at concentrations as low as 50 μM for Fyn SH2 (*10*), 163 μM for phospholipase Cγ1 SH2 (*8*), and 500 μM for Hck SH2 (*11*). Since most NMR results on SH2 domains have been acquired at concentrations of at least 1 mM, interpretation of the results must also consider the dynamics of dimer (and possibly higher-order multimer) formation and dissociation.

Mass Spectrometry of Intact SH2. Mass spectra of intact SH2 were acquired with a Micromass Platform mass spectrometer coupled to capillary perfusion HPLC. First, ten μL (650−700 pmol) of quenched SH2 sample (pH 2.5, 0 °C) was injected into a 100 mm × 0.25 mm i.d. perfusion column (POROS 10 R2 media, PerSeptive Biosystems) operating at a flow rate of 40 μL/min. Then, the protein was eluted with a gradient of 15−98% acetonitrile in 3.5 min. The injector and column were cooled to 0 °C to minimize deuterium back-exchange. With each set of samples, an undeuterated control and a totally deuterated control were also analyzed to adjust for deuterium back-exchange during analysis (*32*). Results obtained for the reference samples of SH2 showed that 90% of the deuterium located at peptide amide linkages was retained during analysis. The HPLC step was performed with protiated solvents, thereby removing deuterium from side chains and amino/carboxy termini that exchange much faster than amide linkages (*33*). Therefore, an increase in molecular mass was a direct measure of the deuteration at peptide amide linkages. Multiple analyses were performed for each time point.

Analysis of Pepsin Fragments of SH2. Deuterium exchange was performed as described above. Immediately before analysis, 10 μL (400−450 pmol) of each sample was incubated with 3 μL of a 2 μg/μL pepsin solution for 5 min at 0 °C. The resulting peptides were separated in 7 min by a 5−60% acetonitrile/water gradient using reversed phase perfusion HPLC. The undeuterated and deuterated controls (as above) were also digested and used to adjust for loss of deuterium from the peptides during analysis. The digests

were analyzed by HPLC/MS under conditions permitting 85% recovery of deuterium at peptide amide linkages. Peptic cleavage sites are difficult to predict from sequence alone but are reproducible under identical digestion conditions. Therefore, all peptides were identified with a combination of analysis of molecular weight information (*32, 34*), MS/MS techniques (*35*), and carboxy-terminal sequencing (*36, 37*). Analyses of SH2 peptides were performed with a Micromass Autospec high-resolution mass spectrometer (AutoSpecETOFFPD) equipped with a focal plane detector and a standard electrospray interface. Data were processed by centroiding an isotopic distribution corresponding to the +1, +2, or +3 charge state of each peptide. Deuterium levels were plotted versus the exchange time and fitted with a series of first-order rate terms according to eq 1 where D is the number of deuterium present, N is the number of peptide amide linkages in a segment, and the k_i are hydrogen−deuterium exchange rate constants for each peptide linkage (*38*). The exchange rate constants, k_i, were varied to obtain

$$D = N - \sum_{i=1}^{N} \exp^{-k_i t}$$

the best fit between the experimental data and eq 1.

RESULTS AND DISCUSSION

Hydrogen Exchange and Protein Dynamics. Hydrogen exchange rates have been used in many studies to investigate changes in the stabilities and dynamics of proteins (e.g., refs *18, 21,* and *39*−*42*). The details of hydrogen exchange mechanisms have been widely reviewed (*43*−*50*). To summarize, the rate constant for isotope exchange at each individual amide linkage in a normally folded protein, k_{ex}, can be described by eq 2

$$k_{ex} = k_f + k_u = (\beta + K_{unf})\, k_2 \qquad (2)$$

where k_{ex} is expressed as the sum of the contributions of exchange from folded (k_f) and unfolded (k_u) forms of the protein (*46*). Equation 2 can be expanded to express k_{ex} as a function of β, K_{unf}, and k_2 where β is the probability for exchange from folded forms (a function of several parameters, including solvent accessibility and intramolecular hydrogen bonding), K_{unf} is the equilibrium constant describing the unfolding process, and k_2 is the rate constant for HX at each amide linkage in an unstructured peptide, a value that can be calculated (*33*). Recent HX/NMR studies have used denaturants to distinguish between β and K_{unf} (*51*−*53*).

Structural changes required for HX described by k_f and k_u differ in the magnitude of atomic displacements required for isotope exchange. Because of the highly compact nature of proteins in their native state, exchange at individual sites is believed to involve small atomic movements, probably around 1 Å, but sufficient to allow diffusion of OD^- and D_2O to the exchange site (*46, 47*). In parallel with this highly local motion, short segments as well as the entire backbone of a protein can exchange through unfolding processes. Molecular motions associated with the unfolding of large segments of the backbone require displacing many atoms several angstroms from their equilibrium positions in the native structure, and global unfolding requires gross movement of the entire backbone. Thus, exchange from the folded form (k_f) of a protein involves primarily low-amplitude motions (small displacement), while exchange from unfolded forms (k_u) requires much larger amplitude motions. Results of a theoretical study by Miller and Dill suggest that large structural changes with little changes in free energy are possible, but uncommon (*48*).

In the discussion that follows, it will be assumed that binding-induced changes in the isotope exchange rates of rapidly exchanging NHs correlate with exchange directly from the folded protein, signifying changes in low-amplitude motion. The validity of this assumption is based on the observation that proteins generally have some amide hydrogens that exchange at rates comparable to those expected for exchange from peptides. According to eq 2, such high-isotope-exchange rates are possible only if β or K_{unf} approaches 1. From typical unfolding free energies in the absence of denaturants (a few kcal/mol), the maximum population of unfolded states is less than a few percent. Since K_{unf} is much less than 0.01 for native conditions, amide hydrogens that undergo isotope exchange at rates comparable to those of peptides likely do so from the folded protein. Because exchange from the folded protein is correlated with low-amplitude motions, binding-induced alterations in exchange of the most rapidly exchanging amide hydrogens in SH2 indicate differences in low-amplitude motion. Although the notion that fast isotope exchange is due primarily to hydrogen exchange from folded proteins is not new, HX/MS is the first practical means of measuring fast hydrogen/deuterium exchange (*25*) (we note that fast hydrogen exchange can be measured with NMR saturation transfer experiments (*54*−*56*) but that this does not involve deuterium/hydrogen exchange). In contrast, since both β and K_{unf} may be small (less than 0.01), binding-induced changes in slow exchange cannot be attributed specifically to changes in small- or large-amplitude motion.

HX/MS Analysis of Intact SH2 Free and Bound to YEEI. To determine how peptide binding affects the motions of SH2, we have examined the hydrogen exchange rates of intact Hck SH2 versus Hck SH2 bound to the 12-residue high-affinity peptide, YEEI. The molecular weight of SH2 was determined by HPLC/MS following incubation of SH2 alone or bound to peptide YEEI in D_2O for 10 s to 8 h. Any deuterium located in side chains was replaced with protium during the HPLC step (see Materials and Methods). As a result, the molecular weight of deuterium-labeled SH2 indicates the number of deuteriums specifically located at peptide amide linkages. The deuterium level in SH2 increased with incubation time, as illustrated in Figure 1, until approximately 71 of the amide hydrogens had been replaced with deuterium. Since Hck SH2 has a total of 102 peptide amide hydrogens, it is evident that 31 of these hydrogens did not exchange, even after incubation in D_2O for 8 h. Because the only previous HX/MS study of an SH2 domain (*23*) was performed without back-exchanging deuterium from amino acid side chains and without buffer, our results cannot be compared quantitatively.

The change in deuterium level with incubation time was fitted with a first-order rate expression (eq 1) to estimate rate constants for isotope exchange at peptide amide linkages. These results are presented in Table 1 as groups of amide hydrogens with similar exchange rates. The error in deter-

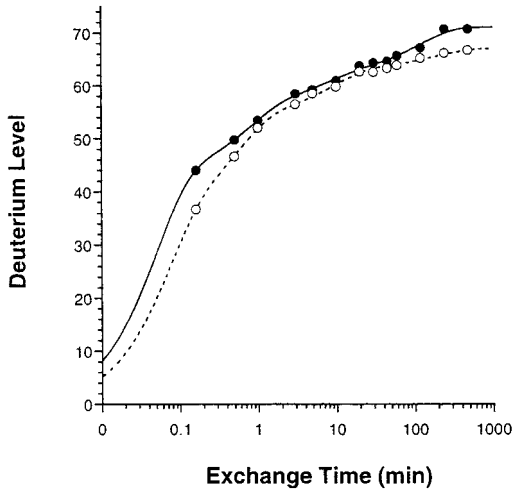

FIGURE 1: The deuterium level found in intact SH2 (●) and intact SH2 incubated with peptide YEEI (○) is shown versus the exchange time (10 s to 8 h). The exchange data were fitted with eq 1 to produce the smooth lines.

Table 1: Distribution of Rate Constants for Isotope Exchange at Peptide Amide Linkages in Hck SH2 Free and Bound to Peptide YEEI

	number of amide hydrogens[a]			
	$k > 10$ min^{-1}	$k \sim 1$ min^{-1}	$k \sim 0.1$ min^{-1}	$k < 0.01$ min^{-1}
SH2	43	13	15	31
SH2 + YEEI	35	19	13	35

[a] The number of peptide amide linkages with hydrogens whose isotope exchange rates are described by the given rate constant was determined by fitting eq 1 to the results presented in Figure 1.

mining the sizes of the groups is approximately ±2 NH for the most rapidly exchanging amide hydrogens and ±1 NH for other categories. Results presented in Table 1 indicate that binding of SH2 to YEEI decreased the number of hydrogens exchanging with $k > 10$ min^{-1} by 8 and increased the number exchanging with $k \sim 1$ min^{-1} by a similar number. Binding to YEEI also increased the number of NH groups that exchange very slowly ($k < 0.01$ min^{-1}). The shift in populations of these categories points to a general decrease in the amount of isotope exchange that occurs in the presence of YEEI.

Differences in hydrogen exchange when SH2 is bound to YEEI are due to a combination of changes in SH2 dynamics and solvent shielding by the peptide. Because of the relatively small size of the peptide, it can shield only a small region of SH2 from the deuterated solvent. The surface area of SH2 occluded by binding an 11-residue peptide to Src SH2 is 410 Å^2 (*3*). Calculations of the accessible surface area [according to the ASC/GM software package, (*57*, *58*)] affected by binding the same 11-residue peptide to Lck SH2 (*29*) indicate that approximately 450 Å^2 is obstructed upon binding. Because of the structural similarity of Hck SH2 to Src and Lck SH2, YEEI bound to Hck SH2 should shield approximately the same area. The accessible surface area (*57*, *58*) of Hck SH2 is 7495 Å^2 indicating that the peptide could shield only ~6% of the total surface of Hck SH2. In addition, based on the NMR structure of uncomplexed Hck SH2 (*26*) and the similarity of its binding site to that of Src and Lck SH2, there are about 10 backbone amide hydrogens

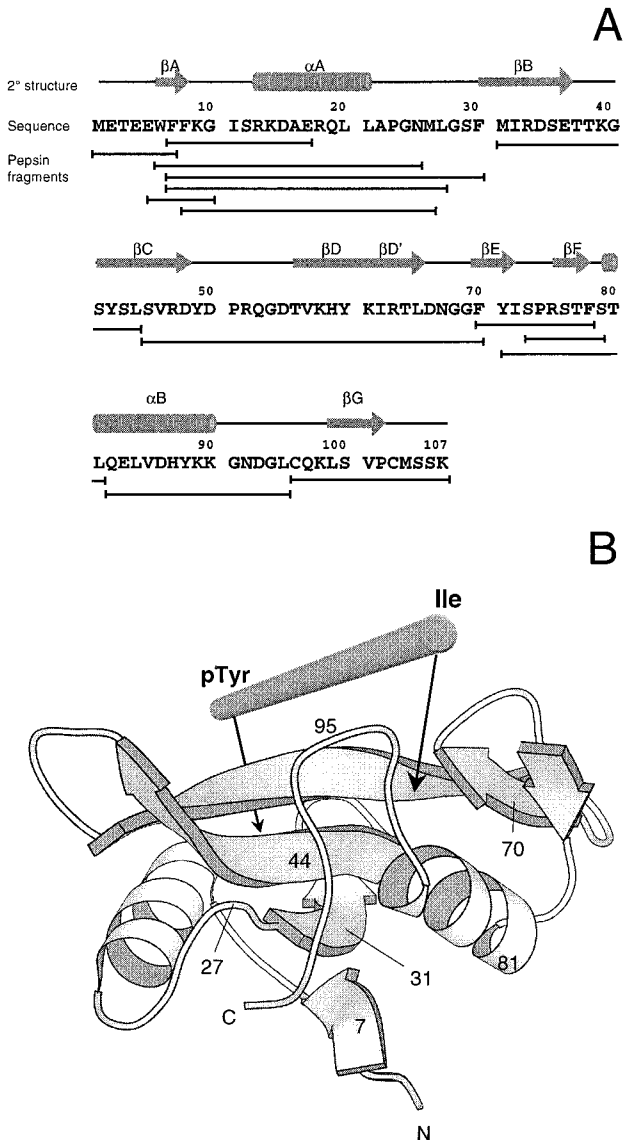

FIGURE 2: Peptic fragments of Hck SH2 aligned with the primary, secondary, and tertiary structure. (A) Peptic fragments of Hck SH2 aligned with the sequence and secondary structural elements. (B) Tertiary structure of Hck SH2 (*11*) indicating the approximate position of the binding peptide and key residues in pepsin digestion.

in and near the binding site that may be significantly shielded by the peptide.

HX/MS Analysis of Peptic Fragments of Free and Bound SH2. To determine how binding affects hydrogen exchange in specific regions of SH2, intact SH2 was labeled as described above but digested into peptides just before analysis by mass spectrometry. Peptic digestion produced 14 fragments that cover 100% of the SH2 backbone (Figure 2). Deuterium levels in short backbone segments of SH2 incubated in D_2O alone or with YEEI were determined from the molecular weights of the corresponding peptic fragments. Typical results are presented in Figure 3 for segments 7−27 and 71−81. Binding of YEEI to Hck SH2 decreases isotope exchange for exposure times less than approximately 1 min in both segments. However, binding decreases slow exchange (exposure time greater than 100 min) substantially in the 7−27 segment and increases slightly slow exchange in the 71−81 segment. The importance of these differences is discussed below.

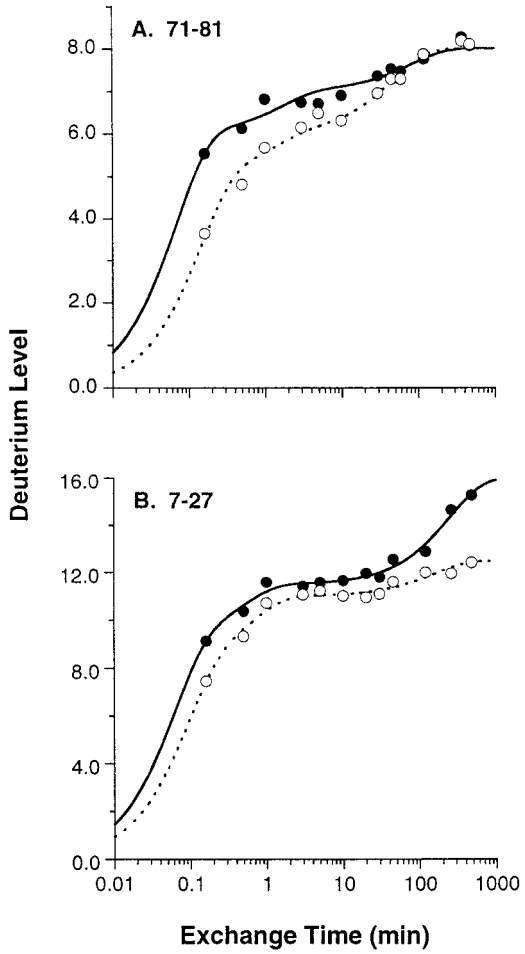

FIGURE 3: Deuterium level found in segments 71−81 (A) and 7−27 (B) of intact Hck SH2 incubated in D_2O (pH 6.9, 22 °C) for 10 s to 8 h in the absence (●) and presence (○) of peptide YEEI. The solid lines were drawn by fitting parameters in eq 1 to the experimental results.

The amide hydrogen at each peptide linkage in the peptic fragments of SH2 has a unique rate constant for isotope exchange. Although specific exchange rate constants have not been determined for each amide hydrogen, the range and distribution of rate constants can be estimated by fitting parameters in first-order rate expressions (eq 1) to the experimental results. Analysis of the 14 peptic fragments used in this study showed that the hydrogen exchange results could be adequately fitted by a four-compartment model in which the amide hydrogens in each fragment were grouped according to their exchange rates (as in Table 2). For the exchange times used in this study, 10 s to 8 h, only those rate constants in the range 0.001−4 min^{-1} could be determined. However, by observing changes in the populations of the four categories upon binding, we classify 92% of the backbone amide hydrogens (exclusive only of those amide hydrogens at the N-termini of each peptide). The fast category includes amide hydrogens with exchange rate constants in the 0.2−4.0 min^{-1} range, while the slow category includes amide hydrogens with exchange rate constants in the 0.001−0.2 min^{-1} range. The categories of very fast and very slow include amide hydrogens that exchange either too fast (k_{ex} > 4 min^{-1}) or too slow (k_{ex} < 0.001 min^{-1}) to be measured for the exchange conditions used in this study.

Table 2: Distribution of Rate Constants for Isotopic Exchange of Hydrogens Located at Peptide Amide Linkages Estimated by Fitting Deuterium Exchange Results Presented in Figure 3 to a Series of Exponential Terms

	category[b]			
segment[a]	very fast	fast	slow	very slow[c]
7−27	9.0 (>4.0)	2.5 (2.1)	4.5 (0.004)	3.0 (<0.001)
7−27 bound	8.0 (>4.0)	3.0 (1.6)	1.5 (0.006)	6.5 (<0.001)
71−81	6.0 (>4.0)	1.0 (0.60)	1.0 (0.01)	1.0 (<0.001)
71−81 bound	5.0 (>4.0)	1.0 (0.77)	2.0 (0.021)	1.0 (<0.001)

[a] See Figure 2 for identification of the segments. [b] The number of amide hydrogens exchanging with the rate constant (min^{-1}) indicated in parentheses. [c] The number of very slow NHs was determined by subtracting the number of NHs exchanged in 8 h from the total number of NHs in each segment.

Results presented in Figure 3 and Table 2 for segments 7−27 and 71−81 illustrate how binding of peptide YEEI to SH2 alters both slow and fast exchange in these segments of the SH2 backbone. Fitting the results with the four-compartment model for segment 7−27 (Figure 3B) shows that ligation decreases the number of amide hydrogens with exchange rates greater than 4 min^{-1} (the very fast group) by one. This result suggests that β decreased substantially for one residue in this segment, consistent with a reduction in low-amplitude motion near this residue. Likewise, the number of NH groups with apparent exchange rate constants of approximately 0.005 min^{-1} (the slow group) decreased by three. The number of NH groups in this segment with exchange rate constants less than 0.001 min^{-1} (the very slow group) increased by 3.5, suggesting that binding decreased exchange of 3−4 of the slowly exchanging NH in the segment including residues 7−27. Similar analysis of results for the segment including residues 71−81 suggests a general reduction in small-amplitude motion with binding.

This approach to detecting changes in dynamics induced by peptide binding to SH2 has been applied to eight peptic fragments that collectively represent the entire SH2 backbone (see Figure 2). Results of this analysis are presented in Figure 4 where the number of amide hydrogens exhibiting similar exchange rates is plotted versus their apparent common exchange rate constant. The number of amide hydrogens that exchange in the very fast category (i.e., k_{ex} > 4 min^{-1}) is indicated on the right of each panel, while the number of amide hydrogens with very slow exchange rates is indicated on the left of each panel. Interpretation of this presentation can be illustrated using results for the 7−27 segment. Binding to YEEI causes a large increase in the number of amide hydrogens that exchange too slowly to be measured, as indicated by the two data points on the left side of the figure. The two data points on the right side of the figure indicate that there is a small decrease in the number of amide hydrogens undergoing very fast isotopic exchange as a result of binding. Changes in the number of amide hydrogens in the fast and slow groups (as well as their apparent exchange rate constants) are illustrated by the two pairs of data points in the middle of the figure. There is little change in the number and apparent rate constant of amide hydrogens in the fast group upon binding of YEEI to SH2, while the number of amide hydrogens in the slow group decreases substantially upon binding.

Binding appears to cause a different type of change in SH2 dynamics in the region, including residues 96−107. In

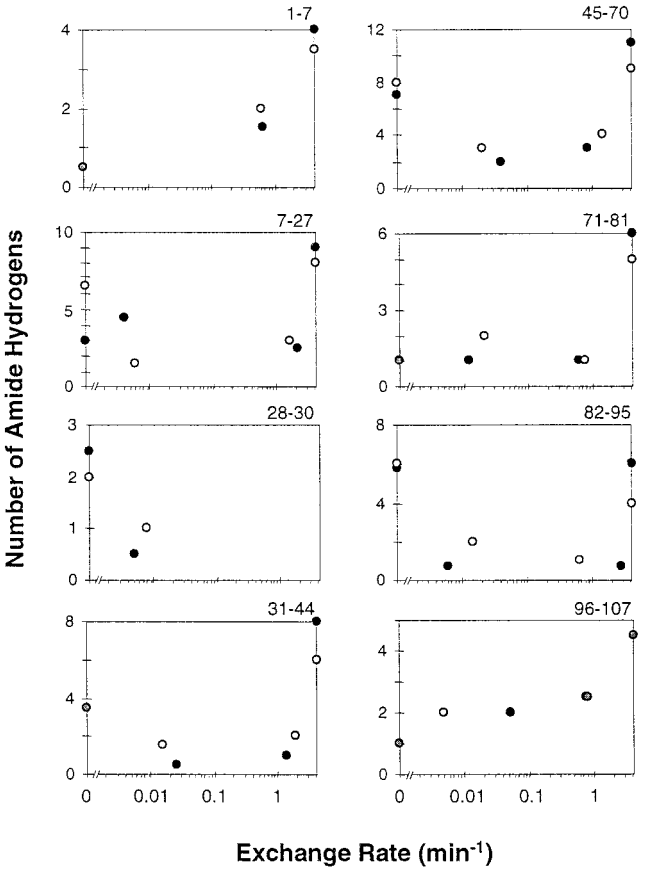

FIGURE 4: Distribution of amide hydrogen exchange rates in peptic fragments covering the entire SH2 backbone. For each segment, the number of amide hydrogens with similar exchange rates is displayed versus their mean exchange rate, SH2 alone (●) and SH2 + YEEI (○). Results were obtained by fitting parameters in eq 1 to deuterium exchange results (e.g., Figure 3). Results for segment 28−30 were determined from the differences in deuterium levels found in overlapping peptic fragments. A gray symbol is used when the solid and open symbols overlap.

this region, the number of residues in all four groups did not change with binding. However, the apparent rate constant for the slow category decreased 10-fold, suggesting that two residues in this region spend much less time in the exchange competent state (a state in which exchange is likely due to unfolding or high β values) when SH2 is bound to the peptide. Since this form of analysis indicates only the distribution of exchange rate constants in a segment of the SH2 backbone, specific peptide linkages included in the groups defined by fitting have not been identified. Hence, two amide hydrogens with slow exchange rates in free SH2 may not be the same hydrogens placed in this category by fitting data for the complex. Despite this ambiguity, the display of results in Figure 4 illustrates how the distribution of isotope exchange rates within short segments of the backbone of SH2 changes with binding to the peptide.

Location of Changes in Dynamics. Figure 5 correlates the primary and secondary structure of Hck SH2 to changes in exchange upon binding to YEEI. The location of each segment in the tertiary structure of SH2 is shown in Figure 2B. The change in the number of amide hydrogens in each segment that exchange in the very fast and very slow categories under the present experimental conditions is presented. Little or no change in the number of slowly exchanging hydrogens was found in segments, including residues 1−7, 28−44, 71−81, or 82−107, suggesting that peptide binding does not change the number of residues exhibiting very slow isotope exchange in these regions. Segments 7−27 and 45−70 show the largest increase in the number of amide hydrogens that exchange only very slowly when SH2 binds to the peptide. Segment 7−27 contains helix αA and a random coil while segment 45−70 contains a large portion of the central β-sheet and is oriented perpendicular to bound YEEI. On the basis of the crystal structure of Src SH2, segment 7−27 has only one contact with peptide YEEI, pY, while segment 45−70 has three contacts, pY, pY + 1, and pY + 3 (*3*). Although some reduction in isotope exchange may be due to shielding by the peptide, the change in segment 7−27 is too large to be attributed to the one contact point (pY) at Arg 13. These results support the idea that reduced hydrogen exchange in these regions is due primarily to increased protein stability as a result of peptide binding.

The number of amide hydrogens that exchanged very fast under the present conditions either decreased or remained unchanged in all segments upon peptide binding to SH2. The extent of this decrease, which indicates the change in low-amplitude motion along the SH2 backbone, is presented in the lower half of Figure 5. Peptide binding decreased the number of amide hydrogens undergoing rapid exchange in all segments except for those at the N- and C-terminus of SH2 (residues 1−7 and 96−107), suggesting that binding of YEEI decreases low-amplitude motion throughout SH2. Segment 31−44, which includes the BC loop, has been implicated in conformational changes upon ligand binding (*3, 8, 10, 11, 29*), and segment 45−70 has substantial direct contact with the peptide. The number of very fast exchanging NH groups was also reduced in segments 71−81 and 82−95. These segments include many residues involved in binding at the pY + 3 position of YEEI. While large changes in conformation and dynamics have not been observed with NMR (perhaps due to different time regimes for motion detected by NMR and HX) at the pY + 3 site (*11*), our results indicate that there are changes in low-amplitude motions in this region.

Since only 2−4 NHs experience altered HX rates in each peptic fragment upon binding of SH2 to YEEI and because the HX rates for individual amide linkages have not been determined, it could be argued that the data in Figure 5 represent large changes to a few amino acids (those in direct contact with the peptide) or small changes to a number of residues (changes throughout the protein). On the basis of HX/NMR work in other systems, protein−ligand binding alters HX in the protein in one of two ways (*21*): (1) changes are restricted to the binding site area (*14, 19, 21*), or (2) changes are felt throughout the structure (*16−18, 59, 60*). We believe the later to be true for SH2. Some changes, such as that seen for segment 7−27, are too large to be attributed to changes only in the binding site. Further, the majority of segment 7−27 is located on the furthest side of SH2 from the binding site for YEEI (see Figure 2B). Additionally, NMR evidence (*11*) has indicated that peptide binding generally reduces motions throughout the domain on a time scale consistent with the measurements made by HX/MS.

Restrictions on the Time Scale for SH2 Dynamics. Mass spectra of intact SH2 or peptic fragments of SH2 (labeled intact) provide two types of information, isotope patterns and

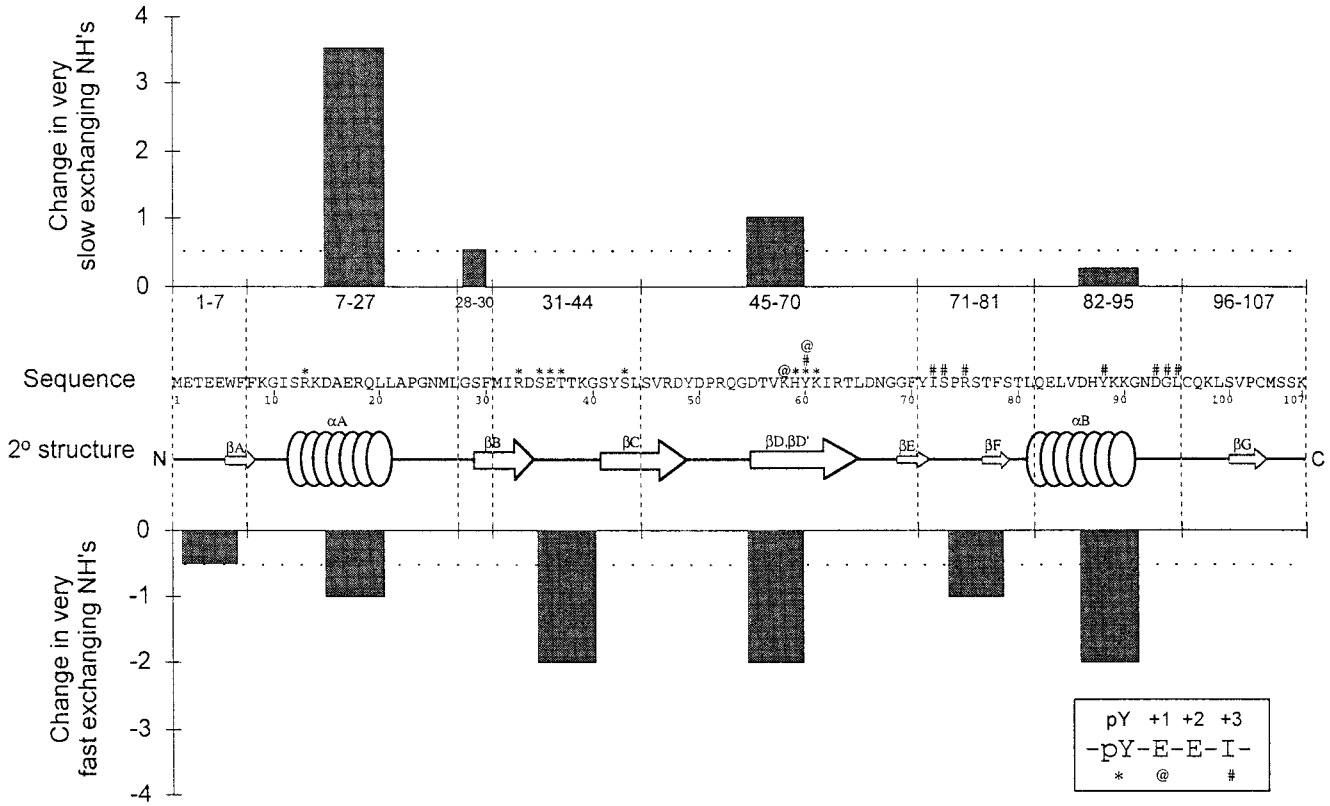

FIGURE 5: Changes in the populations of amide hydrogens in very fast and very slow categories for segments representing the entire SH2 backbone correlated with secondary structure. The absolute number of amide hydrogens that exchange in the very slow category for a given fragment is shown above the secondary structure, while the number of amide hydrogens that are decreased in the very fast category is shown below. Values beyond the dotted lines are significant changes, while those within the lines are within experimental error. The sequence and secondary structure as well as the sites of interaction of YEEI [based on the Src SH2 crystal structure (*3*)] are also shown.

average molecular masses. Isotope patterns are a direct measure of the intermolecular distribution of deuterium, while molecular masses give the deuterium levels. The intermolecular distribution of deuterium is a direct measure of the cooperativity of isotope exchange (e.g., EX1 versus EX2 kinetics), which may correlate with cooperative motion within specific regions of a protein backbone. Cooperative isotope exchange has been used to detect cooperativity in protein folding (*40, 61, 62*) and protein unfolding (*24, 63, 64*). When cooperative exchange prevails, the mass spectra have bimodal isotope patterns and the relative intensities of the two envelopes of isotope peaks are a direct measure of the population of folded and unfolded molecules. None of the isotope patterns in the mass spectra of the 14 peptic fragments used in the present study were bimodal, indicating that hydrogen exchange in Hck SH2 is not cooperative (i.e., does not occur near the EX1 limit). The single binomial isotope distributions found in this study indicate that EX2 kinetics prevail. Since the rate constant for intrinsic hydrogen exchange, k_2, for the present experimental conditions is approximately 1 s^{-1} (calculated from ref *33*), it follows that the refolding rate constants for these 14 SH2 segments are much greater than 1 s^{-1}. If the rate of refolding was 1 s^{-1} or slower, bimodal isotope patterns would be evident.

Detecting Exchange from the Folded Form. The average molecular masses of the peptic fragments indicate the deuterium levels in the SH2 peptic fragments. The change in the deuterium level with incubation time has been used to determine the distribution of hydrogen exchange rate constants within the peptic fragments (this study and refs *32, 38,* and *42*). The distribution of hydrogen exchange rate constants within short segments, as illustrated for segments 7−27 and 71−81 in Table 2, provides an alternate means for detecting cooperative motion in proteins because it may indicate whether hydrogen exchange occurs from the folded or unfolded forms of SH2. Since exchange from the folded form requires, by definition, very localized motions facilitating exchange at only a single amide hydrogen, it follows that exchange rates of amide hydrogens within a short segment depend on the magnitude of β, which may be very different for adjacent residues (*39*). Because β can vary widely, exchange from the folded form results in a wide distribution of exchange rates (k_2) within a given segment. On the other hand, hydrogen exchange from unfolded forms involves, by definition, cooperative motion that renders all of the amide hydrogens in an unfolding segment available for exchange at the same time. The range of HX rate constants of amide hydrogens within an unfolding segment is typically much narrower than the distribution of HX rate constants for exchange from the folded state. Hydrogen exchange from amide positions in cooperatively unfolded states is assumed to occur at nearly the same rates as HX for residues in a totally unstructured peptide with the same sequence. The theoretical distribution of exchange rates for any sequence can be calculated (*33*) and compared with the experimentally determined distribution. It is noted that, although neither the size nor the boundaries of units involved in cooperative motions are known in SH2, results from other proteins suggest that unfolding units include 10−20 residues (*41, 63, 65*). Thus, peptic fragments with 5−20 residues,

such as those produced in peptic digestion of Hck SH2, likely span only one or two cooperative unfolding units and do not introduce artifactually wide distributions.

The presentation of results in Figure 4 demonstrates the wide range of rates at which amide hydrogens located in the same peptic fragment undergo isotopic exchange. Except for the one short segment including residues 28−30, the other peptic fragments have 6−24 amide hydrogens. The majority of amide hydrogens in each of these segments has exchange rate constants that are either very fast ($k_{ch} > 4$ min^{-1}) or very slow ($k_{ch} < 0.001$ min^{-1}). The rate constants, therefore, span a range of greater than 1000. The calculated rate constants for exchange from unfolded forms of most of these fragments, k_2, span a range of only 10. Because the experimentally determined range of isotope exchange rate constants within short segments of the backbone is much wider than the calculated range for these same fragments under these experimental conditions, exchange from the folded form is an important process along the entire SH2 backbone.

Comparison with NMR. The dynamics of different SH2 domains have been investigated by NMR. Results on the phospholipase Cγ1 SH2 domain showed little change in dynamics on the pico- to nanosecond time scale but may have implicated slower conformational movements (*8*). The SH2 domain from the p85 subunit of phosphatidylinositol 3-kinase (PI3K) showed a marked decrease in hydrogen exchange rates upon addition of a tight binding peptide, which was interpreted as stabilization of the folded form (*66*). NMR relaxation data on the PI3K SH2 domain implied movements of the domain on the micro- to millisecond time scale (*67*) but not on the nanosecond time scale (*68*). NMR studies on Hck SH2 and YEEI (*11*), the same system investigated in this study, have indicated a reduction in protein motion on the nano- to pico second time scale. Combining our hydrogen exchange/mass spectrometry data with NMR data gives access to motions ranging from minutes to picoseconds, thus creating a powerful combination for studying the movements of proteins over a wide time scale.

We interpret the hydrogen exchange results presented herein to indicate a generalized shift of the entire SH2 domain toward slower hydrogen exchange with binding to the peptide. These results imply reduced flexibility over much of the domain. Results from NMR show a similar reduction in motion on the pico- to nanosecond time scale. The percent of residues in each peptic fragment of Hck SH2 that have altered average order parameters (S^2) in the presence of YEEI peptide is shown in Figure 6A. Most segments have increased S^2 in the presence of the peptide, and only some segments have minor decreases in S^2, indicating that motions on the pico- to nanosecond time scale are restricted in the presence of peptide. This conclusion is consistent with our data from HX/MS, demonstrating that very fast exchange, which is indicative of low-amplitude motions, is decreased upon binding. Additionally, the number of residues that require an R_{ex} term to fit the NMR relaxation data decreases in the presence of peptide YEEI (Figure 6B) for most segments. The requirement of the R_{ex} term is generally interpreted as reflecting slow conformational exchange of the residue [others have noted that R_{ex} could arise from changes in the chemical environment as a result of motion of vicinal residues (*8*) or motion of nearby aromatic rings (*69*)]. Our

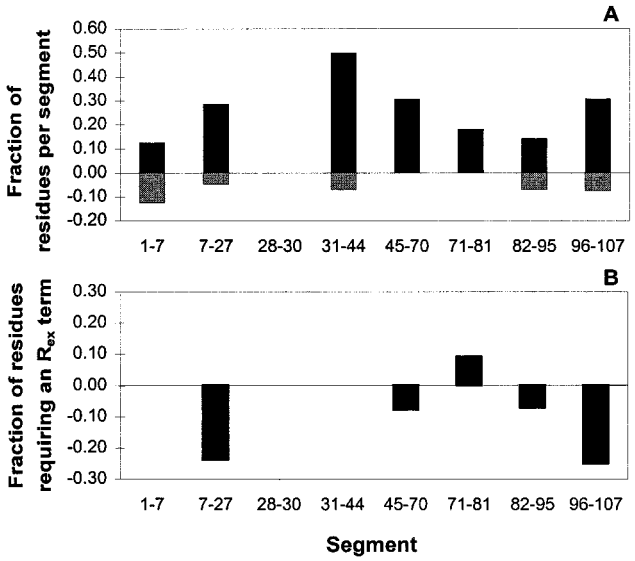

FIGURE 6: NMR results on SH2 dynamics. (A) Change in the average order parameter (S^2) in each segment of SH2. The fraction of residues within each segment that have greater S^2 values in the presence of YEEI is indicated by a positive value (black), and the fraction of residues within a segment that show a decrease in S^2 is indicated as negative (gray). (B) The fraction of residues requiring an R_{ex} term per segment in the presence of YEEI is shown for each segment. A negative value indicates that fewer residues in the bound form require R_{ex} terms to fit the relaxation data.

HX/MS results suggest that motions on a slower time scale are inhibited in the presence of peptide, a view consistent with R_{ex} terms reflecting slow conformational change.

CONCLUSIONS

Measuring exchange rates for rapidly exchanging amide hydrogens is a unique capability of mass spectrometry that allows detection of changes in low-amplitude motions along the protein backbone. Hydrogen exchange and mass spectrometry results have shown that the Hck SH2 domain undergoes a decrease in its backbone dynamics upon peptide binding. Finding no evidence for exchange via EX1 kinetics shows that the lifetimes of the open states is less than 1 s. Results of this study show that the increased rigidity accompanying binding of the high-affinity YEEI peptide to Hck SH2 likely extends throughout the entire protein. Decreases in the number of amide hydrogens that exchange very fast imply a reduction in low-amplitude motion with binding.

These results may have implications in the regulation of protein tyrosine kinases via SH2 domains. All SH2 domains are not in the same environment when they are subunits of larger proteins. Therefore, conformational flexibility of a particular SH2 domain in a particular parent protein may be important for regulation. Perhaps for Hck, binding of the regulatory C-terminal tail of Hck causes an alteration in the conformational flexibility of SH2. A reduction in conformational flexibility within SH2 may do two things. First, it may compensate for low affinity of the tail peptide. As a separate peptide, the C-terminal regulatory sequence has a low affinity for Hck SH2 (*70*). Second, a less flexible SH2 domain may have additional interactions with the rest of the protein. Additional interactions with other parts of the tertiary environment may help lock the kinase in the inactive state.

This may be due to communication of reduced SH2 flexibility to the SH3 domain, an event that may increase the affinity of the SH3 domain for its regulatory sequence, the SH2-kinase linker and favor the inactive state.

REFERENCES

1. Pawson, T., and Schlessinger, J. (1993) *Curr. Biol. 3*, 434−442.
2. Cohen, G. B., Ren, R., and Baltimore, D. (1995) *Cell 80*, 237−248.
3. Waksman, G., Shoelson, S. E., Pant, N., Cowburn, D., and Kuriyan, J. (1993) *Cell 72*, 779−790.
4. Lipari, G., and Szabo, A. (1982) *J. Am. Chem. Soc. 104*, 4546−4559.
5. Lipari, G., and Szabo, A. (1982) *J. Am. Chem. Soc. 104*, 4559−4570.
6. Kördel, J., Skelton, N. J., Akke, M., Palmer, A. G. I., and Chazin, W. J. (1992) *Biochemistry 31*, 4856−4866.
7. Nicholson, L. K., Kay, L. E., Baldisseri, D. M., Arango, J., Young, P. E., Bax, A., and Torchia, D. A. (1992) *Biochemistry 31*, 5253−5263.
8. Farrow, N. A., Muhandiram, R., Singer, A. U., Pascal, S. M., Kay, C. M., Gish, G., Shoelson, S. E., Pawson, T., Forman-Kay, J. D., and Kay, L. E. (1994) *Biochemistry 33*, 5984−6003.
9. Kay, L. E., Muhandiram, D. R., Farrow, N. A., Aubin, Y., and Forman-Kay, J. D. (1996) *Biochemistry 35*, 361−368.
10. Pintar, A., Hensmann, M., Jumel, K., Pitkeathly, M., Harding, S. E., and Campbell, I. D. (1996) *Eur. Biophys. J. 24*, 371−380.
11. Zhang, W., Smithgall, T. E., and Gmeiner, W. H. (1998) *Biochemistry 37*, 7119−7126.
12. Akke, M., and Palmer, A. G. (1996) *J. Am. Chem. Soc. 118*, 911−912.
13. Pedersen, T. G., Thomsen, N. K., Andersen, K. V., Madsen, J. C., and Poulsen, F. M. (1993) *J. Mol. Biol. 230*, 651−660.
14. Paterson, Y., Englander, S. W., and Roder, H. (1990) *Science 249*, 755−759.
15. Benjamin, D. C., Williams, D. C., Smith-Gill, S. J., and Rule, G. S. (1992) *Biochemistry 31*, 9539−9545.
16. Williams, D. C., Jr., Benjamin, D. C., Poljak, R. J., and Rule, G. S. (1996) *J. Mol. Biol. 257*, 866−876.
17. Werner, M. H., and Wemmer, D. E. (1992) *J. Mol. Biol. 225*, 873−889.
18. Loh, S. N., Prehoda, K. E., Wang, J., and Markley, J. L. (1993) *Biochemistry 32*, 11022−11028.
19. Meiering, E. M., Bycroft, M., Lubienski, M. J., and Fersht, A. R. (1993) *Biochemistry 32*, 10975−10987.
20. Orban, J., Alexander, P., and Bryan, P. (1994) *Biochemistry 33*, 5702−5710.
21. Kragelund, B. B., Knudsen, J., and Poulsen, F. M. (1995) *J. Mol. Biol. 250*, 695−706.
22. Robinson, C. V., Chung, E. W., Kragelund, B. B., Knudsen, J., Aplin, R. T., Poulsen, F. M., and Dobson, C. M. (1996) *J. Am. Chem. Soc. 118*, 8646−8653.
23. Anderegg, R. J., and Wagner, D. S. (1995) *J. Am. Chem. Soc. 117*, 1374−1377.
24. Engen, J. R., Smithgall, T. E., Gmeiner, W. H., and Smith, D. L. (1997) *Biochemistry 36*, 14384−14391.
25. Dharmasiri, K., and Smith, D. L. (1996) *Anal. Chem. 68*, 2340−2344.
26. Zhang, W., Smithgall, T. E., and Gmeiner, W. H. (1997) *J. Biomol. NMR 10*, 263−272.
27. Sicheri, F., Moarefi, I., and Kuriyan, J. (1997) *Nature 385*, 602−609.
28. Zhang, W., Smithgall, T. E., and Gmeiner, W. H. (1997) *FEBS Lett. 406*, 131−135.
29. Eck, M. J., Shoelson, S. E., and Harrison, S. C. (1993) *Nature 362*, 87−91.
30. Payne, G., Shoelson, S. E., Gish, G. D., Pawson, T., and Walsh, C. T. (1993) *Proc. Natl. Acad. Sci. U.S.A. 90*, 4902−4906.
31. Morelock, M. M., Ingraham, R. H., Betageri, R., and Jakes, S. (1995) *J. Med. Chem. 38*, 1309−1318.
32. Zhang, Z., and Smith, D. L. (1993) *Protein Sci. 2*, 522−531.
33. Bai, Y., Milne, J. S., Mayne, L., and Englander, S. W. (1993) *Proteins: Struct., Funct., Genet. 17*, 75−86.
34. Zhou, Z., and Smith, D. L. (1990) *J. Protein Chem. 9*, 523−532.
35. Biemann, K. (1990) *Methods Enzymol. 193*, 455−479.
36. Caprioli, R. M., and Fan, T. (1986) *Anal. Biochem. 154*, 596−603.
37. Smith, J. B., Sun, Y., Smith, D. L., and Green, B. (1992) *Protein Sci. 1*, 601−608.
38. Zhang, Z., Post, C. B., and Smith, D. L. (1996) *Biochemistry 35*, 779−791.
39. Kim, K.-S., Fuchs, J. A., and Woodward, C. K. (1993) *Biochemistry 32*, 9600−9608.
40. Miranker, A., Robinson, C. V., Radford, S. E., Aplin, R. T., and Dobson, C. M. (1993) *Science 262*, 896−900.
41. Bai, Y., Sosnick, T. R., Mayne, L., and Englander, S. W. (1995) *Science 269*, 192−197.
42. Zhang, Z., and Smith, D. L. (1996) *Protein Sci. 5*, 1282−1289.
43. Hvidt, A., and Nielsen, S. O. (1966) *Adv. Protein Chem. 21*, 287−385.
44. Woodward, C., Simon, I., and Tüchsen, E. (1982) *Mol. Cell. Biochem. 48*, 135−160.
45. Englander, S. W., and Kallenbach, N. R. (1984) *Q. Rev. Biophys. 16*, 521−655.
46. Kim, K.-S., and Woodward, C. (1993) *Biochemistry 32*, 9609−9613.
47. Elber, R., and Karplus, M. (1987) *Science 235*, 318−321.
48. Miller, D. W., and Dill, K., A. (1995) *Protein Sci. 4*, 1860−1873.
49. Clarke, J., Itzhaki, L. S., and Fersht, A. R. (1997) *TIBS 22*, 284−287.
50. Smith, D. L., Deng, Y., and Zhang, Z. (1997) *J. Mass Spectrom. 32*, 135−146.
51. Bai, Y. W., Milne, J. S., Mayne, L., and Englander, S. W. (1994) *Proteins: Struct., Funct., Genet. 20*, 4−14.
52. Itzhaki, L. S., Neira, J. L., and Fersht, A. R. (1997) *J. Mol. Biol. 270*, 89−98.
53. Chamberlain, A. K., and Marqusee, S. (1998) *Biochemistry 37*, 1736−1742.
54. Hodsdon, M. E., and Cistola, D. P. (1997) *Biochemistry 36*, 2278−2290.
55. Gryk, M. R., Finucane, M. D., Zheng, Z., and Jardetzky, O. (1995) *J. Mol. Biol. 246*, 618−627.
56. Gryk, M. R., and Jardetzky, O. (1996) *J. Mol. Biol. 255*, 204−214.
57. Eisenhaber, F., and Argos, P. (1993) *J. Comput. Chem. 14*, 1272−1280.
58. Eisenhaber, F., Lijnzaad, P., Argos, P., Sander, C., and Scharf, M. (1995) *J. Comput. Chem. 16*, 273−284.
59. Mau, T., Baleja, J. D., and Wagner, G. (1992) *Protein Sci. I*, 1403−1412.
60. Skelton, N. J., Koerdel, J., Akke, M., and Chazin, W. J. (1992) *J. Mol. Biol. 227*, 1100−1117.
61. Heidary, D. K., Gross, L. A., Roy, M., and Jennings, P. A. (1997) *Nat. Struct. Biol. 4*, 725−731.
62. Yang, H., and Smith, D. L. (1997) *Biochemistry 36*, 14992−14999.
63. Deng, Y., and Smith, D. L. (1998) *Biochemistry 37*, 6256−6262.
64. Zhang, Z., Li, W., Li, M., Logan, T. M., Guan, S., and Marshall, A. G. (1997) *Technol. Protein Chem. 8*, 703−713.
65. Milne, J. S., Mayne, L., Roder, H., Wand, A. J., and Englander, S. W. (1998) *Protein Sci. 7*, 739−745.

66. Shoelson, S. E., Sivaraja, M., Williams, K. P., Hu, P., Schlessinger, J., and Weiss, M. A. (1993) *EMBO J. 12*, 795−802.
67. Breese, A. L., Kara, B. V., Barratt, D. G., Anderson, M., Smith, J. C., Luke, R. W., Best, J. R., and Cartlidge, S. A. (1996) *EMBO J. 15*, 3579−3589.
68. Hensmann, M., Booker, G. W., Panayotou, G., Boyd, J., Linacre, J., Waterfield, G., and Campbell, I. D. (1994) *Protein Sci. 3*, 1020−1030.
69. Constantine, K. L., Friedrichs, M. S., Goldfarb, V., Jeffrey, P. D., Sheriff, S., and Mueller, L. (1993) *Proteins: Struct., Funct., Genet. 15*, 290−311.
70. Bibbins, K. B., Boeuf, H., and Varmus, H. E. (1993) *Mol. Cell. Biol. 13*, 7278−7287.

BI982611Y